A DFT Protocol for the Prediction of 31 P NMR Chemical Shifts of Phosphine Ligands in Transition Metal Complex- es

Pierre-Adrien Payard, Luca Alessandro Perego, Laurence Grimaud, Ilaria Ciofini

A DFT Protocol for the Prediction of ³¹P NMR Chemical Shifts of Phosphine Ligands in Transition Metal Complexes

Pierre-Adrien Payard,*[a] ‡ Luca Alessandro Perego,*[a][b] ‡ Laurence Grimaud[a] and Ilaria Ciofini*[b]

[a] Laboratoire des Biomolécules, LBM, Département de Chimie, École Normale Supérieure, PSL University, Sorbonne Université, CNRS, 75005 Paris, France. [b] PSL Research University, Institute of Chemistry for Health and Life Sciences, ICLeHS, CNRS-Chimie ParisTech, 11 rue P. et M. Curie, F-75005 Paris 05 (France).

DFT • ³¹P NMR • phosphine • basis set • first row organometallic compounds • theoretical prediction

ABSTRACT: While ³¹P NMR is a major technique to characterize phosphine-ligated transition metal complexes - which are ubiquitous in catalysis - ³¹P NMR chemical shifts are difficult to predict using empirical rules or tabulated data. Aiming at filling this gap, we propose here guidelines enabling their prediction at a modest computational cost. Rooted in DFT (Density Functional Theory), our protocol features structural optimization and magnetic shielding tensor calculations performed at a global hybrid level using a tailored locally dense basis set. Validation on an experimental data series revealed that while a careful conformational analysis is required in the case of flexible phosphines, the use of the free ligand or another complex as a reference for chemical shifts often allows to solve this drawback. Applicability to various diamagnetic complexes of first-row transition metals is demonstrated, including large systems relevant to contemporary catalysis.

In organometallic and coordination chemistry, ³¹P NMR is a key spectroscopy to disclose the structural features of metal complexes having phosphorus ligands. This tool is routinely used for the characterization of stable compounds as well as to evidence short-lived reaction intermediates.[1] Therefore, this technique is particularly useful to elucidate the mechanisms of catalytic reactions and to aid in the development of new transformations[2] promoted by phosphine-ligated metal catalysts.[1a] Indeed, ³¹P nuclei usually yield easily observable and sharp NMR signals over a wide chemical shift range, providing valuable chemical information due to their high sensitivity even to minor structural changes.[1a] Unfortunately, while the chemical shifts of ¹H or ¹³C in organic molecules has been traditionally estimated by the use of empirical correlation tables,[3] ³¹P NMR chemical shifts are notoriously difficult to predict based only on qualitative considerations and tabulated data.[1, 4] Indeed, whereas ¹H and ¹³C NMR spectroscopies are mainly concerned with contributions due to σ-bonding or to well-defined and recurring πbonded structural elements, the influence of π-bonding in ³¹P NMR is larger in magnitude, more frequent and less transferable from one compound to another, thus preventing the development of predictive empirical rules.[1b]

In the last decades, however, the estimation of ¹H and ¹³C NMR shielding constants by using density functional theory (DFT) emerged and imposed as a very reliable and computationally affordable tool to support the structural elucidation of complex organic molecules.[5] By contrast, the use of DFT to predict ³¹P NMR chemical shifts has not yet been validated extensively.[6] Van Wüllen first used DFT methods to calculate ³¹P chemical shift using both IGLO and GIAO approaches on a series of small molecules.[6b] Maryasin and co-workers described a protocol based on the use of a GIAO in conjunction with a rather large basis set (6-311++G(2d,2p)).[6e] It seems however that a lower level of theory may be efficient as well:[6d, 6n] Latypov and co-workers suggested "smaller" basis sets such as 6-31G(d) may be efficient in most of the cases.[6n] Non-specific and specific solvent effects,[6f] such as hydrogen bonding, were also investigated.[6o] Indeed, the use of DFT approaches allows to handle large systems such as polyoxometalates.[6m] More recently, the case of solid state ³¹P NMR has also been examined.[6p] As we were writing these lines, Latypov and

co-workers reported a study on the applicability of DFT to predict the ³¹P NMR chemical shifts of model nickel complexes based on small/medium-sized organophosphorus ligands.[7]

The development of an easily handled and reliable routine method would be of great help to assist structural assignments, particularly in the case of complexes featuring multiple phosphine, in the case of complex mixtures of products, or to complete the characterization of non-isolable reaction products and intermediates.[6j, 6l]

The aim of the present work is to establish and validate a DFT protocol based on the GIAO approach for the prediction of solution (isotropic) ³¹P NMR chemical shifts of diamagnetic first-row transition metal complexes. Due to the comparative abundance of data available in the literature for nickel-phosphine complexes, Ni containing complexes were predominantly selected to build a benchmark set suitable to validate our computational approach. Moreover, nickel-based catalytic systems are currently under active development.[8]

The full training set of complexes analyzed in this work is reported in Figure 1 (for the complete tables of chemical shifts of complexes and associated references, see the Supporting Information, Tables S1-S2). This series contains a variety of Ni(0) complexes (**1-18**) and Ni(II) complexes (complexes **19-21**). It is complemented by a few complexes of other transition metals (Cr(0), Cu(I), Mo(0) and W(0), complexes **22-25**).

First, the computational method was established by using a subset of six simple Ni(0) PMe₃-ligated complexes (Figure 1, complexes **1-6**). Since the chemical shift is critically dependent on the geometry of the complexes, we determined the level of theory needed both for structural optimizations and for magnetic shielding tensor calculations. The resulting methodology was then validated on a larger number of compounds using the full training set depicted in Figure 1. Finally, some concrete examples of application of our protocol to identify intermediates and off-cycles species in the case of "real-life" catalytic cycles are presented in the last part of this paper, including diamagnetic complexes of transition metals other than nickel (Fe(II) and Mn(I)).
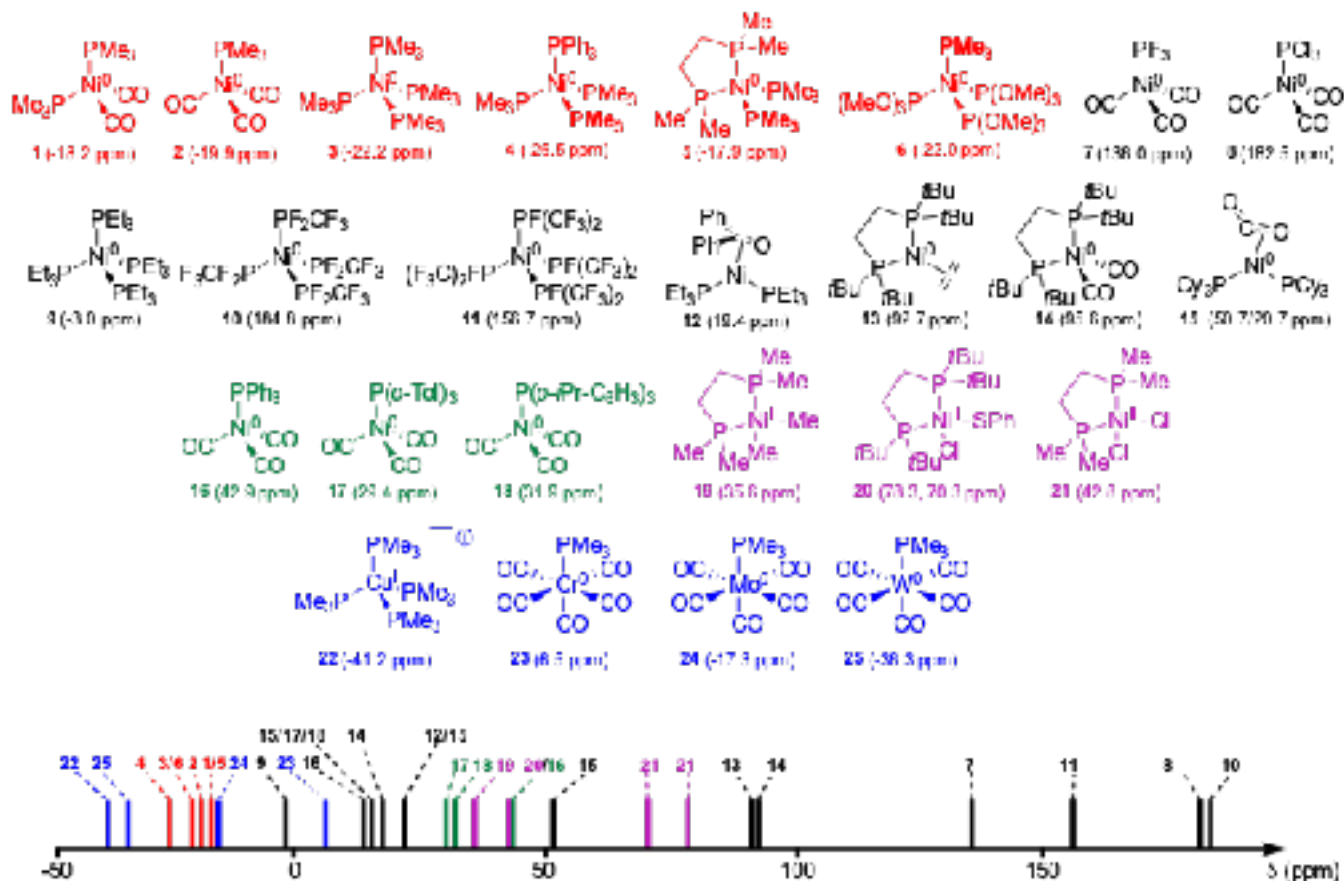
Figure 1. Structures and experimental ^{31}P isotropic chemical shifts of the training set of complexes used in this study. In red are reported the Ni(0) complexes used to setup the computational protocol (**1-6**), in black the Ni complexes used to validate it (**7-15**), and in green some Ni(0) complexes that are discussed more in detail due to tri-aryl phosphine peculiar conformational issues (**16-18**), in violet Ni(II) complexes which deserve special care due to various degree of paramagnetic character (**19-21**), in blue complexes of metals other than Ni (**22-25**). Experimental ^{31}P NMR chemical shifts in solution are indicated in parentheses. See the Supporting Information, Table S2 for literature references and details of the conditions in which the spectra were recorded. When more than one inequivalent phosphorus nucleus is present, only the one highlighted in boldface was included in the analysis. *o*-Tol = *o*-Me-C₆H₄.

Results and Discussion

We recall that the chemical shift (δ_X) of a nucleus X is defined as: $\delta_X = \sigma_{ref} - \sigma_X + \delta_{ref}$ where σ_{ref} and σ_X are the NMR isotropic magnetic shielding constants of a reference nucleus and of the nucleus X respectively and δ_{ref} is the chemical shift of a reference nucleus with respect to a primary reference (for the complete table of calculated isotropic magnetic constants of complexes and free phosphines see the Supporting Information, Tables S3-S4). In the case of ^{31}P NMR, the zero of the scale ($\delta_{ref} = 0$) is a solution of orthophosphoric acid (H₃PO₄, 85% in water). Considering the difficulties to model this system, PH₃[6b, 6m] or PPh₃[6e] were proposed as "secondary standards" to reference computed chemical shifts.[6e] It may also be advantageous to choose different reference compounds for nuclei of the same kind residing in qualitatively different chemical environments. An analogous concept has already been applied to the prediction of ^{13}C NMR chemical shifts: the use of two different reference molecules, one for sp³-hybridized and one for sp and sp²hybridized carbons allows indeed to reduce the error.[9]

In our case, we are particularly interested in the prediction of the change in chemical shift associated to the formation of the metal-phosphorus bond. This variation can be defined as $\delta_{LP} - \delta_{FP} = \sigma_{FP} - \sigma_{LP}$ where δ_{LP} and δ_{FP} are the chemical shifts of the phosphorus nucleus in the metal-bound and free ligand respectively and σ_{LP} and σ_{FP} are the corresponding isotropic shielding constants. Indeed, the chemical shift of the free phosphine (δ_{FP}) is normally known and excess free

ligand may be present in the analyzed solution and used as a secondary reference standard. Thus, the ^{31}P chemical shift of the phosphine in the metal complex can be rewritten as $\delta_{LP} = \sigma_{FP} - \sigma_{LP} + \delta_{FP}$.

Setup and Validation of the computational approach

Experimental studies on series of structurally related complexes, highlighted that the metal-phosphorus bond length[10] and the cone angle of the phosphine[11] have a critical effect on the chemical shift.[12] As a consequence, obtaining reliable geometries is a pre-requisite to predict ^{31}P NMR chemical shift. The Ni-P bond length and the Ni-P-C angle were chosen as indicators to judge the convergence of the computational protocol for structural predictions focusing first on complex **1** (Figure 1).In order to setup a cost-effective method, we decided to fix the exchange correlation functional to the popular global hybrid B3LYP[13] and to screen different basis set combinations so as to obtain adequately accurate convergence of the geometric parameters at a modest computational cost. Solvent effects were accounted for with the PCM model, using the parameters of the solvent used for experimental measurements (for both optimization and NMR calculations; see the Supporting Information, Table S2 for literature references and details of the conditions (solvent) in which the spectra were recorded).

First, we analyzed the effect of the basis set on the metal atom. We considered the Los-Alamos family of basis and pseudo potential for the Ni atom and tested the LANL2DZ and LANL2TZ basis sets.[26] Starting with the triple-zeta Los-Alamos basis set (LANL2TZ) used with the associated pseudo-poten-

tial (LANL2), addition of diffuse (LANL2TZ+) or f-polariza-tion functions (LANL2TZ(f)) lead to less than 1 mÅ change in the Ni-P bond length (see the Supporting Information, Table S5). By contrast, using the smaller LANL2DZ basis set lead to a variation of more than 20 mÅ. To estimate the impact of bond length on the isotropic shielding constant, a scan of σ along the Ni-P distance in complex **1** was performed. A modi-fication of 1 mÅ induced a change of less than 0.1 ppm (see the Supporting Information, Figure S1), which validates the choice of LANL2TZ/LANL2 to describe Ni for geometry op-timization.
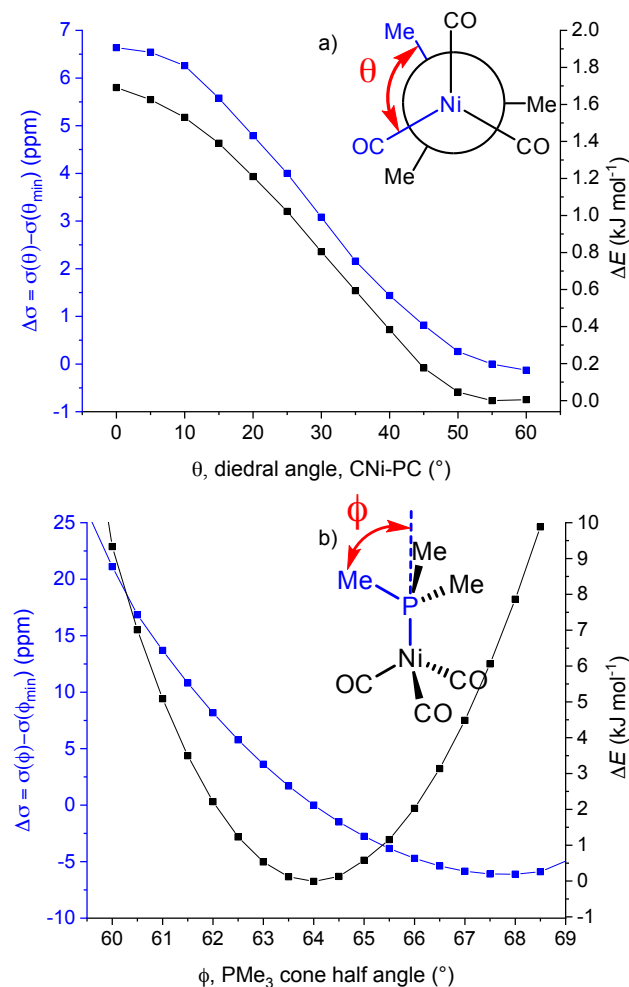

Figure 2. a) Energy scan (ΔE) for rotation of PMe₃ (θ = CNi-PC dihedral angle) around the Ni-P bond axes in complex **2** (right scale, black curve) and the associated evolution of ³¹P NMR iso-tropic shielding tensor (left scale, blue curve, $\Delta\sigma = \sigma(\theta) - \sigma(\theta_{min})$, with θ_{min} the minimal energy angle). b) Energy scan (ΔE) for change in the PMe₃ cone angle (ϕ) in complex **2** (right scale, black curve) and the associated evolution of ³¹P NMR isotropic shielding tensor (left scale, blue curve, $\Delta\sigma = \sigma(\phi) - \sigma(\phi_{min})$, with ϕ_{min} the minimal energy angle). ³¹P NMR shielding constants were evaluated at the B3LYP(GIAO)/BS2 level of theory.

Similarly, the effect the basis set on P and O on the optimized Ni-P bond length and P-Ni-P angle was studied (see the Sup-porting Information, Table S6). In this case split-valence Pople basis sets (double or triple zeta) were evaluated. Starting with 6-31G, addition of diffuse functions (6-31+G) resulted in a noticeable change of the bond length (–61 mÅ). By contrast, the addition of d-polarization functions (6-31+G(d)) had only a negligible impact. Changing from double to triple zeta basis (6311+G(d)) does not significantly affect the results. Conse-

quently, the B3LYP functional in conjunction with LAN2TZ/ LANL2 on Ni, 6-31+G(d) on P, O and other atoms, and 6-31G(d) on C and H have been retained as computational protocol for structural optimization. Hereafter this composite basis set will be referred to as BS1. All optimized structures are reported in the Supporting Information, §4 Cartesian coor-dinates and absolute energies).

Another caveat with the structural optimization of phosphine and phosphine-metal complexes is the possibility of populat-ing several conformations at room temperature. Indeed, a con-formational analysis and a subsequent Boltzmann average was necessary for the prediction of the chemical shift of flexible phosphites.[6e] For instance, if we consider the very simple structure of complex **2** (Figure 1), there could be free rotation around the Ni-P bond and the cone angle of the phosphine may also vary. To estimate the influence of these effects on the isotropic shielding tensor, a scan of σ along the C-P-Ni-P di-hedral was performed (Figure 2a). A 60° rotation of trimethylphosphine corresponds to a variation of σ of more than 6 ppm.[14] This process is predicted to be nearly barrierless and thus may have a significant impact on the chemical shift. Using a Boltzmann distribution and sampling conformations with a 5° rotation step, the chemical shift is indeed shifted downfield of 1.5 ppm compared to the chemical shift comput-ed for minimal energy configuration.

The effect of the cone angle in complex **2** on the chemical shift was also investigated. As described in the literature[11] the effect of the cone angle on the isotropic shielding tensor is relevant (more than 60 ppm for a 15° distortion, see the Sup-porting Information Figure S2). If we consider only the struc-tures accessible at room temperature (Figure 2b, correspond-ing to less than 10 kJ mol⁻¹ for a variation of 5°) the variation of the isotropic shielding tensor in this area is more than 25 ppm. Using a Boltzmann-averaged sampling, the predicted chemical shift changed by nearly 1 ppm compared to the most stable staggered conformation. An analogous calculation on free PMe₃ (see the Supporting Information, Figure S3) re-vealed a very similar behavior and the contribution to the chemical shift due to a variation of the cone angle is of the same order of magnitude (0.9 ppm). This may be explained by considering that in complex **2** the steric hindrance due to the interaction with the CO ligands is very weak and thus the pos-sible deformations of the ligated phosphine are similar to those of the free ligand.

Based on these observations, we can conclude that it is advan-tageous to use the corresponding free phosphine as a reference for the calculation of the ³¹P NMR chemical shifts of com-plexes and focus on the difference of chemical shift between the free and ligated phosphine. When the accessible conforma-tional spaces are similar for the free and ligated phosphine, no conformational analysis would likely be needed due to trans-ferability of dynamic conformational effects between the free and the metal-bound ligand. On the contrary, the rotation of the phosphine around the metal-P axis (a degree of freedom not relevant for the free phosphine) should be checked if ther-mally accessible.

The choice of the basis set for the calculation of the NMR shielding tensor was then examined. The use of unbalanced, "locally dense" basis sets for the cost-effective calculation of ¹³C NMR chemical shifts in large organic molecules at the Hartree-Fock level was first proposed by Chesnut and Moore.[15] In this approach, high quality large basis set are employed only on the atom for which the NMR chemical shift is to be calculated, while computationally cheaper basis sets are used to describe all the other atoms.[16] Its applicability in conjunc-tion with post-HF methods has been investigated later,[17] and this subject has been reexamined in a systematic fashion for the case of peptides recently.[18] In our case, the "locally dense" basis set concept would allow significant saving of computa-

tional time, especially for large metal complexes featuring multiple phosphorus ligands.

We investigated the suitability of this approach for metal complexes at DFT level. Thus, we kept the basis set employed for geometry optimization for all atoms but the P atom of interest and we investigated the effect of the basis on the latter. In this respect, we considered the family of the polarization consistent basis sets with segmented contraction pcsSeg-x (x = 0–3), which was designed by Jensen to describe the core properties of nuclei.[19] This basis set family proved to be particularly efficient for NMR calculations.[19]
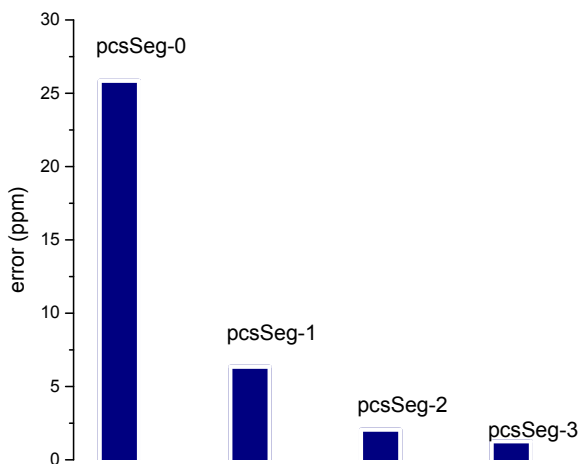

Figure 3. Error on the chemical shift calculated for complex **3** (with respect to experimental values), using polarization consistent basis sets with segmented contraction on the P atom of interest (pcSseg-x, x = 0, 1, 2 and 3) with the GIAO method, and the B3LYP functional. The following basis set was used for the other nuclei: LANL2TZ-LANL2 (Ni), 6-31G(d) (C and H), 6-31+G(d) (other P atoms).

Using the B3LYP functional in combination with the GIAO approach, the absolute error on the chemical shift of complex **3** (Figure 3) converged to less than 1 ppm using the pcsSeg-3 basis set on the P nucleus of interest (Figure 3, the 6-31+G(d) basis set was employed for the other three P centers). The B3-LYP functional was selected on the grounds of previous studies revealing its efficiency in calculation of NMR shielding tensors.[6d] Differently from what demonstrated for related systems,[20] the PBE0 functional did not significantly outperform B3LYP (see the Supporting Information, Figure S4).

The effect of the basis set on the other atoms was also investigated. Addition of diffuse functions to describe C and H significantly improves the results while addition of d-polarization functions is detrimental (see the Supporting Information, Table S8). Going from a double zeta basis set to a triple zeta did not lead to any significant improvement (see the Supporting Information, Tables S8) while sizably increasing the computational cost. Concerning P atoms other than that of interest, both d-polarization and diffuse functions are needed (see the Supporting Information, Table S9). The following composite basis set was selected and it will be referred as BS2 in the following: pcsSeg-3 on the P nucleus of interest, 6-31G(d) on C and H atoms, 6-31+G(d) on any other atoms (including P centers other than that of interest).

Finally, we assessed the magnitude of solvent effects modelled using polarization continuum model (PCM, refer to Computational Details). The ^{31}P chemical shift of complex **3** varied of about 2 ppm passing from benzene to acetonitrile, which is in agreement with previous reports[6e, 6f] (see the Supporting Information, Figure S5) and of comparable magnitude with the

accuracy of our method (*vide infra*). We decided to keep PCM solvation for the rest of this study, as it does not significantly increase the computational cost.

Table 1. Experimental and calculated ^{31}P chemical shift (ppm) of complexes 1-6, PMe3 was used as a secondary reference ($\delta = \sigma_{PMe3} - \sigma + \delta_{PMe3}$).

Complex	1	2	3	4	5	6
Exp.	-18.2	-19.9	-22.2	-26.5	-17.9	-22.2
Calc.	-18.3	-17.4[a]	-23.5	-25.2	-15.1	-20.7
Abs. error	0.1	2.5	1.3	1.3	2.8	1.5

[a] Before Boltzmann correction related to free rotation (*vide supra*, Figure 2a): -16.3 ppm. With correction corresponding to free rotation (no Boltzmann-weighed averaging): -18.0 ppm. With Boltzmann-averaged correction -17.4 ppm.

The optimized protocol was then tested on complexes **1** to **6** (Table 1) and proved to be efficient in the prediction of chemical shifts. Indeed, based on geometric optimization at the B3-LYP/BS1 level and subsequent NMR calculation at the GIAO-B3LYP/BS2 level (*vide supra* the definition of BS1 and BS2 composite basis sets), it was possible to predict the chemical shift of these species with an average unsigned error of 1.6 ppm.

Scope and limitations

The efficiency of the method optimized on a small subset of Ni(0), PMe3-ligated complexes was then further tested on a larger set (Table 2, Figure 1) including various phosphine-type ligands (complexes **7-18**, PF3, PCl3, PEt3, PF2CF3, PF(CF3)2, PCy3, PPh3, P(o-Tol), P(*o-i*Pr-C6H4)3, bidentate phosphines), Ni(II) complexes (complexes **19-21**) and finally complexes of other metals (complexes **22-25**, Cu(I), Cr(0), Mo(0), W(0)).

Varying the nature of the phosphine did not drastically influence the accuracy of the prediction. However, in the case of highly flexible phosphines such of PEt3 (complex **9**) or PF2CH3 (complex **10**) the absolute error increased, thus suggesting the importance of conformational analysis and dynamics in these instances.[6e]
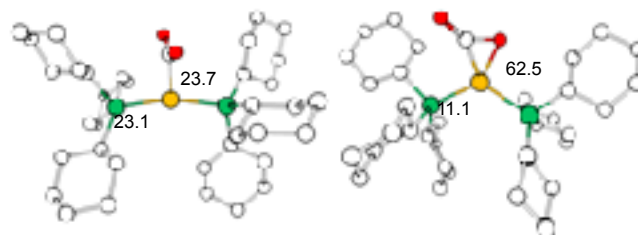

Figure 5. Conformation of complex **15** [Ni(η2-CO2)(PCy3)2], calculated ^{31}P chemical shifts are indicated (Ni atom in yellow, P atoms in green, O atoms in red, C atoms in white, H atoms omitted for clarity). PCy3 was used as a secondary reference ($\delta = \sigma_{PCy3} - \sigma + \delta_{PCy3}$).

Two different conformations can be optimized for [Ni(η2-CO2)(PCy3)2] (complex **15**, Figure 5), a complex relevant for activation of CO2. The first displays orthogonal PNiP and OCO planes while the latter shows coplanar PNiP and OCO. In the latter case, the two phosphorus centers are not equivalent. While this structure is predicted to possess two resonances at 11.1 and 62.5 ppm, the latter would have a single signal at 23

ppm (Figure 5). Experimentally, the spectra of this complex features two signals at 20.7 and 50.7 ppm in ^{31}P NMR, matching with the second structure. This conclusion is in agreement with the computed thermodynamics, since the second geometry is predicted to be favored by 24.6 kJ mol^{-1}.

The case of aryl phosphine was studied in detail (*vide infra*) due to their relevance as ligands in catalysis. The prediction of the ^{31}P chemical shift of complexes of aromatic phosphines is especially difficult due to their conformational freedom.[6e, 21] The case of P(*o*-Tol)₃ has been analyzed in depth (complex **17**).

estimated at only 7 kJ mol^{-1} (Figure S7). Two minimal energy structures are obtained, corresponding to the conformation with the methyl group outside ("out") or inside ("in") the cone formed by the aryl groups (Figure 4). The "in" conformer is thermodynamically favored by 16 kJ mol^{-1}, consequently only this conformer was considered.
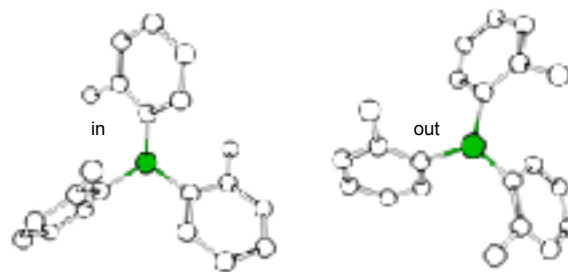

Figure 4. Conformations of P(*o*-Tol)₃ (P atoms in green, C atoms in white, H atoms omitted for clarity).

However, the metal-bound P(*o*-Tol)₃ complex **17** has two nearly isoergonic conformations of the ligand, with the 'in' one slightly favored by 5 kJ mol^{-1}. In this case, both conformations have to be considered to obtain a reasonable estimation of the chemical shift at room temperature (Table 3). Both conformer are separated by more than 20 ppm due to the variation of the cone angle. The same reasoning was successfully applied to the case of (*o*-iPr-C₆H₄)₃P in complex **18** (Table 3).

Changing the oxidation state of the metal from Ni(0) to Ni(II) (complex **19-21**) can affect the accuracy of the approach as evidenced by the values of Table 4. While the chemical shift of complex **19** is described correctly the error become significant for complexes **20** and **21**. This failure can be directly related with the energy gap between singlet and triplet state (ΔG(S→T), Table 4): the lower the triplet energy, the more the error. As already noticed by Latipov and co-workers, residual paramagnetic behavior hampers accurate chemical shift prediction by DFT calculations.[7]

Table 2. Experimental and calculated ^{31}P chemical shift of complexes **7-15**. The associated free phosphine (L) was used as a secondary reference ($\delta = \sigma_L - \sigma + \delta_L$).

Complex	Phosphine (L)	Calculated δ (ppm)	Experimental δ (ppm)	Abs. error (ppm)
7	PF₃	136.5	136.0	0.5
8	PCl₃	176.3	182.5	6.2
9	PEt₃	-8.6	-3.0	5.6
10	PF₂CF₃	170.5	184.8	14.3
11	PF(CF₃)₂	155.1	156.7	1.6
12	PEt₃	19.7	19.4	0.3
13	tBu₂PCH₂-CH₂PtBu₂	86.6	92.7	6.6
14	tBu₂PCH₂-CH₂PtBu₂	89.2	95.6	6.4
15	PCy₃	11.1	20.7	9.6
		62.5	50.7	11.8

Table 4. Experimental and calculated ^{31}P chemical shift of complexes **19-21**. The associated free phosphine (L) was used as a secondary reference ($\delta = \sigma_L - \sigma + \delta_L$).

Complex	Calculated δ (ppm)	Experimental δ (ppm)	Abs. error (ppm)	ΔG(S→T) (kcal mol⁻¹)
19	39.3	35.6	3.7	+17.7
20	70.6	70.3	0.3	+6.7
	97.7	78.3	19.4	
21	42.8	85.5	42.7	+1.9

Table 3. Experimental and calculated ^{31}P chemical shift of complexes **16-18** for different conformations and average values. The associated free phosphine (L) in its most stable conformation ("in") was used as a secondary reference ($\delta = \sigma_L - \sigma + \delta_L$).

	$\Delta_f G_{in/out}$ (kJ mol¹)	Calc. δ - 'out' conformer (ppm)	Calc. δ - "in" conformer (ppm)	Average calc. δ	Exp. shift	Abs. error
16	-	-	-	47.7	42.9	4.8
17	5.5	30.65	18.36	24.5	29.4	4.9
18	5.1	46.15	21.83	33.9	31.9	1.9

Finally, our protocol could also be applied to complexes based on first-row transition metal other than Ni (such as Cu(I) and Cr(0), complexes **22-25**), but it substantially failed at predicting the ^{31}P NMR chemical shifts of complexes of second and third row metals (here exemplified by Mo(0), W(0), complexes **24-25**), likely due to the lack of appropriate treatment of relativistic effects in the chosen model.[6f, 6m]

Rotation of the *o*-Tol groups around the P-C bond can be considered as free at ambient temperature with an energy barrier

Table 4. Experimental and calculated 31P chemical shift of complexes **22-25**. PMe₃ was used as a secondary reference ($\delta = \sigma_{PMe3} - \sigma + \delta_{PMe3}$).

Complex	Metal center	Calculated δ (ppm)	Experimental δ (ppm)	Abs. error (ppm)
22	Cu(I)	-43.4	-47.5	4.1
23	Cr(0)	13.8	6.5	7.3
24	Mo(0)	-2.4	-17.3	14.9
25	W(0)	-4.5	-36.3	31.8

The data from Tables **1-4** were used to plot calculated *vs* experiment chemical shift (Figure 6). Overall our method performs well with a regression coefficient of $R^2 = 0.99$, the slope is very close to one (slope = 0.96). Consequently, no additional affine correction is needed, differently from previous reports.[6n] The average unsigned error was 4.2 ppm, it compares favorably with previously reported methods.[7]
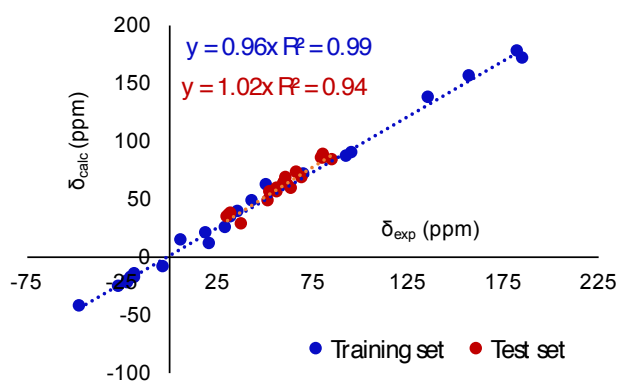

Figure 6. Calculated versus experimental chemical shift of complexes **1-25** (in blue, training set, complexes **21**, **24** and **25** were omitted for above discussed reasons, namely residual paramagneticity and relativistic effects) and complexes **26-37** (in red, test set). Geometries optimized at the B3LYP/BS1 level of theory. 31P NMR shielding constants were evaluated with the GIAO method at the B3LYP/BS2 level of theory.

Application to the structural elucidation of complex catalytic system

To demonstrate the interest of our approach for practical applications, we report here some examples showing how it could assist in the interpretation of experimental 31P NMR spectra.

First, we attempted to discriminate between a mixture of structurally related Ni(II) complexes differentiated by their anionic ligands (Cl *vs* Br *vs* OH), organization (mono *vs* dinuclear form) and, finally, configuration (*trans vs cis*). The complexes selected for this test (Figure 7, Ar = 2-Me-4-F-C₆H₃) were described in a previous work on the mechanism of the nickel-catalyzed Suzuki-Miyaura cross-coupling, in which the role of these species in the catalytic cycle was elucidated.[22] More in details, the interaction of *trans*-[NiArCl(PPh₃)₂] (complex **27**) with Br⁻ and OH⁻ has been described. The variation of the 31P NMR chemical shift upon substitution of the chlorido ligand by a bromido to give *trans*-[NiArBr(PPh₃)₂] (complex **26**, experimental $\Delta\delta$ = +0.8 ppm) is well reproduced by calculations (computed $\Delta\delta$ = +0.6 ppm). Upon addition of OH⁻ to **26**, four new signals at higher field appeared.

Substitution of Br⁻ by OH⁻ may potentially yield either the monomeric complex *trans*-[NiAr(OH)(PPh₃)₂] (**28**) or dimeric

μ-OH bridged complexes [NiAr(μ-OH)(PPh₃)]₂ (**29a-d**). Calculations allow to clearly decide between these two hypotheses: a negative variation of –8 ppm is expected for the monomer *versus* a positive shift of +15 ppm for dimers. Finally, four isomers of [NiAr(μ-OH)(PPh₃)]₂ can be formed (see Figure 6): phosphine ligands may be placed *trans* (**29a-b**) or *cis* (**29c-d**) around the dinuclear core and the *ortho* methyl groups of Ar can be either *anti* (**29b,d**) or *syn* (**29a,c**) with respect to the Ni(μ−OH)₂Ni plane. Complexes featuring the phosphine arranged in a *trans* fashion are predicted to resonate at lower field (37.4 and 38.0 ppm) than complexes with phosphine arranged in a *cis* conformation (34.2 and 36.2 ppm). This trend is in agreement with the experimental observations.[22] Lastly, the calculations allow to put forward an assignment of the signals of all isomers, which could not be deduced from experimental data (Figure 7).
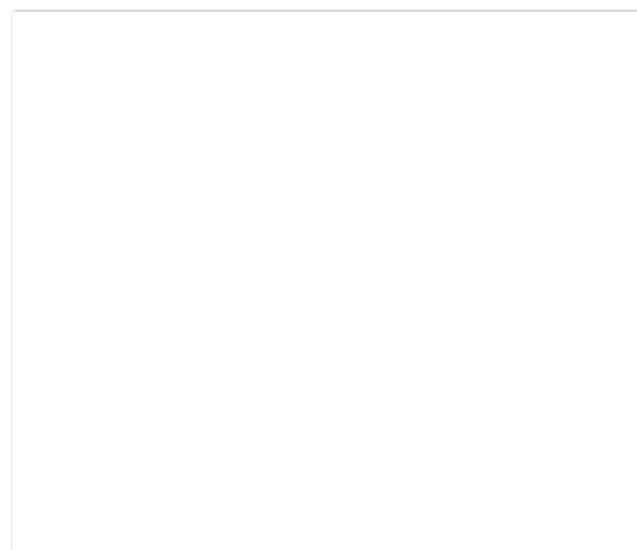
Figure 7. ArNi(II) complexes potentially involved in the catalytic cycle of a Ni-catalyzed Suzuki coupling[23] Experimental[23] (blue) and calculated (red, B3LYP(GIAO)/BS2//B3LYP/BS1 level of theory) chemical shifts are reported. Complex **27** was used as a secondary reference ($\delta = \sigma_{28} - \sigma + \delta_{28}$).

To highlight the applicability of our computational protocol to assist the interpretation of 31P NMR of complexes of first-row transition metal relevant to catalysis, additional systems based on metals other than nickel were examined. The Mn(I) complexes **30a-b** (Figure 8) featuring a P-stereogenic PN(H)P ligand are useful as catalyst for the asymmetric hydrogenation of prochiral ketones.[23] In the context of an investigation of the mechanism of this reaction, several potentials intermediates of the catalytic cycle were prepared and studied by 31P NMR spectroscopy. More in details, treatment of **30** with KH gave a mixture of the amido complex **31**, *syn* hydride **32** and *anti* hydride **33**. Compound **32a** reduced acetophenone to give the diastereoisomeric alcoxo complexes (**S**)-**34a** and (**R**)-**34a**. 31P NMR chemical shifts of these complexes were calculated using our theoretical protocol (Figure 8) taking complexes **30a** (for R = Cy) and **30b** (for R = *t*Bu) as references to anchor the computed chemical shifts, to avoid a burdensome conformational analysis of this flexible ligand. The mean unsigned error of the 11 calculated values was 3.4 ppm, which is in line with the accuracy observed in our benchmark set of Ni complexes. Remarkably higher accuracy was obtained series of complexes with R = *t*Bu (**31-32b**) than for analogues with R = Cy (**31-32a**), most likely due to the reduced conformational freedom of the *t*Bu residue compared to Cy.
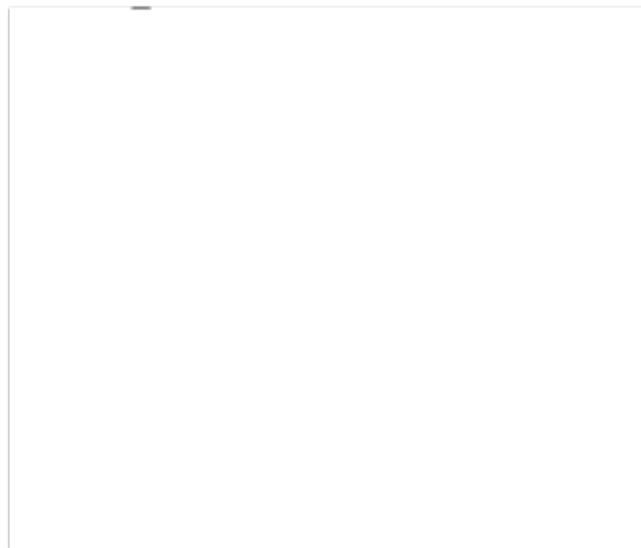
Figure 8. Mn(I) complexes of a P-chiral PNP ligand involved in the asymmetric reduction of prochiral ketones.[23] Experimental[23] (blue) and calculated (red) chemical shifts are reported. Complex **30a** and **30b** were used respectively as a secondary reference for complexes **31-34a** and **31-32b**.

A last example was drawn from the field of iron catalysis, based on a recent report by Mezzetti and coworkers.[24] In the course of the study of the mechanism of the asymmetric transfer hydrogenation of ketones catalyzed by the iron(II) complex [Fe(CNCEt$_3$)$_2$(**L**)](BF$_4$)$_2$ (**L** is a chiral N$_2$P$_2$ macrocycle), the reaction of the hydride complex **35** [FeH(CNEt$_3$)(**1**)](BF$_4$) with acetophenone was studied (Figure 8).[24] A complicated mixture of products containing the diastereoisomeric alkoxo complexes (**S**)-**36** and (**R**)-**36**, and bromo complex **37** (from Br$^-$ present in the reaction medium) was obtained. Application of our procedure to the prediction of the ^{31}P NMR chemical shifts of these species relevant to catalysis (with **35** as the reference compound, 7 computed values, Figure 9) gave a mean unsigned error of 3.8 ppm, which is a performance similar to that observed for the systems discussed previously. This observation suggests that stereochemical analysis of the remote Et$_3$CNC ligand, which has high conformational freedom, is not needed (i.e. this ligand is sufficiently far from the P, so that the detailed description of its conformations is not required to estimate the ^{31}P NMR chemical shifts). Unfortunately, the difference in the chemical shifts of diastereomers (**R**)- and (**S**)-**36** (3.1 ppm in the best case) is so small that the error of the method would not allow to use the calculations to support assignment of the spectra. This example, however, highlights that our computational protocol can be applied to rather large systems (complexes (**R**)- and (**S**)-**36** have 58 non-hydrogen atoms) due to its moderate computational cost, and that no significant loss of accuracy is observed passing from smaller model compounds to these larger systems encountered in modern catalysis. The data presented of Figures 7-9 were added to the calculated versus experimental data plot (red, Figure 6), no difference in behavior was observed with the training set described in the first part of this paper (blue), the average unsigned error was 4.1 ppm, the slope closed to one (1.02) and the regression coefficient is only slightly lower (0.94).
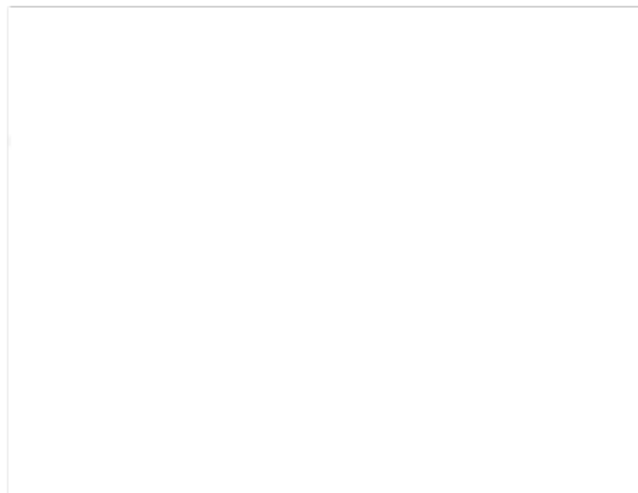

Figure 9. Fe(II) complexes of a chiral P$_2$N$_2$ macrocyclic ligand involved in the asymmetric transfer hydrogenation of prochiral ketones.[24] Experimental[24] (blue) and calculated (red, B3LYP(GIAO)/BS2//B3LYP/BS1 level of theory) chemical shifts are reported. Complex **35** was used as a secondary reference ($\delta = \sigma_{28} - \sigma + \delta_{28}$).

Conclusions

Guidelines enabling the theoretical prediction of ^{31}P NMR chemical shifts of first row transition metal complexes at a modest computational cost have been established. First, adequately accurate geometries are to be obtained. At this end, our protocol employs a global hybrid functional (B3LYP) with a composite basis set (BS1). BS1 comprises a triple zeta basis set with an effective core potential (LAN2TZ/LANL2) on the metal and a double zeta basis set on other atoms (6-31G(d) for C and H, 6-31G+(d) for other atoms). Solvent effects are included using an implicit solvation model (PCM). These resulting optimized structures are submitted to NMR shielding tensor calculation using the GIAO approach with the B3LYP functional and a tailored composite basis set (BS2). BS2 is a composite "locally dense" basis set comprising a triple-zeta quality segmented polarization-consistent basis set (pcs-Seg3) on the P center of interest and double zeta basis set on other atoms (6-31G(d) for C and H, 6-31G+(d) for other atoms). Careful analysis of conformational and dynamic effects on the chemical shift is crucial to obtain reliable results. In the simplest cases, these effects are transferable from the free phosphine to the complex. Consequently, using the free phosphine as a reference to anchor the calculated chemical shifts allows to reduce errors due to systematic error cancelation. In selected cases, however, sampling of conformational space and Boltzmann averaging is recommended. Overall, this procedure allows estimating ^{31}P NMR chemical shifts of diamagnetic complexes featuring different phosphines and first-row metals with errors typically below 3 ppm. This optimized protocol has been applied to catalytically relevant systems and proved particularly robust for the estimation of chemical shift differences of structurally related complexes. In perspective, calculated ^{31}P NMR chemical shifts can be used as a tool to assist spectral assignment of stable complexes and transient catalytic intermediates.

Computational Details

All DFT calculations were performed with the Gaussian09 program (Rev. A.02).[25] The structures of all minima were fully optimized using the B3LYP functional[13] without any symmetry constraint. Basis sets used for structural optimization (BS1: LAN2TZ/LANL2)[26] on Ni, 6-31G(d) on C and H and 6-31+G(d) on all other atoms) and NMR calculation (BS2: pcsSeg-3[19] on the P nucleus of interest, 6-31G(d) on C and H atoms, 6-31+G(d) on any other atoms (including P centers

other than that of interest)) are detailed in the text (section "Setup and Validation of the computational approach). To simulate experimental conditions, bulk solvent effects were accounted for by using an implicit solvation model (IEF-PCM) as implemented in Gaussian, for both geometry optimization and shielding constant calculations.[27] The default spheres radii, static and optical dielectric constants for each solvent were used. All stationary points were characterized as minima by analytical frequency calculations.

ASSOCIATED CONTENT

Supporting Information

A listing of the contents of each file supplied as Supporting Information should be included. For instructions on what should be included in the Supporting Information as well as how to prepare this material for publication, refer to the journal's Instructions for Authors.

The Supporting Information is available free of charge on the ACS Publications website.

AUTHOR INFORMATION

Corresponding Author

*pierre-adrien.payard@ens.fr; luca.perego@ens.fr; ilaria.ciofini@chimie-paris.psl.eu

Author Contributions

‡These authors contributed equally.

ACKNOWLEDGMENT

REFERENCES

(1) (a) Pregosin, P. S.; Kunz, R. W., *31P and 13C NMR of Transition Metal Phosphine Complexes*. Springer-Verlag, Berlin-Heidelberg, **1979**; (b) Kühl, O., *Phosphorus-31 NMR Spectroscopy: A Concise Introduction for the Synthetic Organic and Organometallic Chemist.* Springer-Verlag, Berlin-Heidelberg, **2008**.

(2) (a) Glueck, D. S., Applications of 31P NMR spectroscopy in development of M(Duphos)-catalyzed asymmetric synthesis of P-stereogenic phosphines (M=Pt or Pd). *Coord. Chem. Rev.* **2008**, *252* (21), 2171-2179; (b) Glueck, D. S., Erratum to "Applications of 31P NMR spectroscopy in development of M(Duphos)-catalyzed asymmetric synthesis of P-stereogenic phosphines (M=Pt or Pd)" *Coord. Chem. Rev.* **2011**, 255 (1), 356.

(3) Hesse, M.; Meier, H.; Zeeh, B., *Spectroscopic Methods in Organic Chemistry*, Thieme Verlag, **2007**.

(4) Tong, J.; Liu, S.; Zhang, S.; Li, S. Z., Prediction of 31P nuclear magnetic resonance chemical shifts for phosphines. *Spectroc. Acta A* **2007**, 67 (3), 837-846.

(5) (a) Schreckenbach, G.; Ziegler, T., Density functional calculations of NMR chemical shifts and ESR g-tensors. *Theor. Chem. Acc.* **1998**, 99 (2), 71-82; (b) Barone, G.; Gomez-Paloma, L.; Duca, D.; Silvestri, A.; Riccio, R.; Bifulco, G., Structure Validation of Natural Products by Quantum-Mechanical GIAO Calculations of 13C NMR Chemical Shifts. *Chem. Eur. J.* **2002**, 8 (14), 3233-3239; (c) Smith, S. G.; Paton, R. S.; Burton, J. W.; Goodman, J. M., Stereostructure Assignment of Flexible Five-Membered Rings by GIAO 13C NMR Calculations: Prediction of the Stereochemistry of Elatenyne. *J. Org. Chem.* **2008**, 73 (11), 4053-4062.

(6) (a) Rozhenko, A. B.; Schoeller, W. W.; Povolotskii, M. I., Ab initio calculation of NMR shielding in phosphaalkenes X—P=CY₂. *Magn. Reson. Chem.* **1999**, 37 (8), 551-563; (b) van Wullen, C., A comparison of density functional methods for the calculation of phosphorus-31 NMR chemical shifts. *Phys. Chem. Chem. Phys.* **2000**, 2 (10), 2137-2144; (c) Rezaei-Sameti, M., Ab initio calculations of 31P NMR chemical shielding tensors in alkyl phosphorus compounds and comparison with experimental values. *J. Mol. Structure* **2008**, 867 (1),

122-124; (d) Chernyshev, K. A.; Krivdin, L. B., Quantum-chemical calculations of NMR chemical shifts of organic molecules: I. Phosphines, phosphine oxides, and phosphine sulfides. *Russ. J. Org. Chem.* **2010**, 46 (6), 785-790; (e) Maryasin, B.; Zipse, H., Theoretical studies of 31P NMR spectral properties of phosphanes and related compounds in solution. *Phys. Chem. Chem. Phys.* **2011**, 13 (11), 5150-5158; (f) Chernyshev, K. A.; Krivdin, L. B., Quantum-chemical calculations of NMR chemical shifts of organic molecules: II. Influence of medium, relativistic effects, and vibrational corrections on phosphorus magnetic shielding constants in the simplest phosphines and phosphine chalcogenides. *Russ. J. Org. Chem.* **2011**, 47 (3), 355-362; (g) Chernyshev, K. A.; Larina, L. I.; Chirkina, E. A.; Rozinov, V. G.; Krivdin, L. B., Quantum-chemical calculation of NMR chemical shifts of organic molecules: III. Intramolecular coordination effects on the 31P NMR chemical shifts of phosphorylated N-vinylazoles. *Russ. J. Org. Chem.* **2011**, 47 (12), 1859-1864; (h) Chernyshev, K. A.; Larina, L. I.; Chirkina, E. A.; Rozinov, V. G.; Krivdin, L. B., Quantum-chemical calculations of NMR chemical shifts of organic molecules: IV. Effect of intermolecular coordination on 31P NMR shielding constants and chemical shifts of molecular complexes of phosphorus pentachloride with azoles. *Russ. J. of Org. Chem.* **2011**, 47 (12), 1865-1869; (i) Lantto, P.; Jackowski, K.; Makulski, W.; Olejniczak, M.; Jaszuński, M., NMR Shielding Constants in PH₃, Absolute Shielding Scale, and the Nuclear Magnetic Moment of 31P. *J. Phys. Chem. A* **2011**, 115 (38), 10617-10623; (j) Chernyshev, K. A.; Larina, L. I.; Chirkina, E. A.; Rozinov, V. G.; Krivdin, L. B., Quantum-chemical calculations of chemical shifts in NMR spectra of organic molecules: V. Stereochemical structure of unsaturated phosphonic acids dichlorides from 31P NMR spectral data. *Russ. J. Org. Chem.* **2012**, 48 (5), 676-681; (k) Pudasaini, B.; Janesko, B. G., Evaluation of Approximate Exchange-Correlation Functionals in Predicting One-Bond 31P–1H NMR Indirect Spin–Spin Coupling Constants. *J. Chem. Theor. Comp.* **2013**, 9 (3), 1443-1451; (l) Chernyshev, K. A.; Larina, L. I.; Rozinov, V. G.; Krivdin, L. B., Quantum-chemical calculations of NMR chemical shifts of organic molecules: IX. Electronic structure of [dimethylamino(chloro)methylideneamino]trichlorophosphonium hexachlorophosphate: Azomethine or azophosphine? *Russ. J. Org. Chem.* **2013**, 49 (2), 195-197; (m) Pascual-Borras, M.; Lopez, X.; Poblet, J. M., Accurate calculation of 31P NMR chemical shifts in polyoxometalates. *Phys. Chem. Chem. Phys.* **2015**, 17 (14), 8723-8731; (n) Latypov, S. K.; Polyancev, F. M.; Yakhvarov, D. G.; Sinyashin, O. G., Quantum chemical calculations of 31P NMR chemical shifts: scopes and limitations. *Phys. Chem. Chem. Phys.* **2015**, 17 (10), 6976-6987; (o) Begimova, G.; Tupikina, E. Y.; Yu, V. K.; Denisov, G. S.; Bodensteiner, M.; Shenderovich, I. G., Effect of Hydrogen Bonding to Water on the 31P Chemical Shift Tensor of Phenyl- and Trialkylphosphine Oxides and α-Amino Phosphonates. *J. Phys. Chem. C* **2016**, 120 (16), 8717-8729; (p) Chernyshov, I. Y.; Vener, M. V.; Shenderovich, I. G., Local-structure effects on 31P NMR chemical shift tensors in solid state. *J. Chem. Phys.* **2019**, 150 (14), 144706.

(7) Latypov, S. K.; Kondrashova, S. A.; Polyancev, F. M.; Sinyashin, O. G., Quantum Chemical Calculations of 31P NMR Chemical Shifts in Nickel Complexes: Scope and Limitations. *Organometallics* **2020**, doi 10.1021/acs.organomet.0c00127.

(8) (a) Tasker, S. Z.; Standley, E. A.; Jamison, T. F., Recent advances in homogeneous nickel catalysis, *Nature* **2014**, 509, 299–309 (b) Tasker, S. Z.; Standley, E. A.; Jamison, T. F., Erratum: Recent advances in homogeneous nickel catalysis. *Nature* **2014**, 510, 176-176; (c) Mousseau, J. J.; Charette, A. B., Direct Functionalization Processes: A Journey from Palladium to Copper to Iron to Nickel to Metal-Free Coupling Reactions. *Acc. Chem. Res.* **2013**, 46 (2), 412-424; (d) Han, F.-S., Transition-metal-catalyzed Suzuki–Miyaura cross-coupling reactions: a remarkable advance from palladium to nickel catalysts. *Chem. Soc. Rev.* **2013**, 42 (12), 5270-5298.

(9) Sarotti, A. M.; Pellegrinet, S. C., A Multi-standard Approach for GIAO 13C NMR Calculations. *J. Org. Chem.* **2009**, 74 (19), 7254-7260.

(10) Hunter, A. D.; Williams, T. R.; Zarzyczny, B. M.; Bottesch, H. W.; Dolan, S. A.; McDowell, K. A.; Thomas, D. N.; Mahler, C. H., Correlations among 31P NMR Coordination Chemical Shifts, Ru–P Bond Distances, and Enthalpies of Reaction in Cp′Ru(PR₃)₂Cl

Complexes (Cp′ = η⁵-C₅H₅, η⁵-C₅Me₅; PR₃ = PMe₃, PPhMe₂, PPh₂Me, PPh₃, PEt₃, PnBu₃). *Organometallics* **2016,** 35 (16), 2701-2706.

(11) Carturan, G.; Scrivanti, A.; Longato, B.; Morandini, F., Influence of the phosphine ligands in the ¹H and ³¹P NMR behaviour of [(η³-allyl)Py(phophine)Cl] complexes. *J. Org. Chem.* **1979,** 172 (1), 91-97.

(12) For a more exhaustive discussion about the different structural and electronic effects see reference 1b.

(13) (a) Becke, A. D., A new mixing of Hartree–Fock and local density-functional theories. *J. Chem. Phys.* **1993,** 98 (2), 1372-1377; (b) Lee, C.; Yang, W.; Parr, R. G., Development of the Colle-Salvetti correlation-energy formula into a functional of the electron density. *Phys. Rev. B* **1988,** 37 (2), 785-789; (c) Vosko, S. H.; Wilk, L.; Nusair, M., Accurate spin-dependent electron liquid correlation energies for local spin density calculations: a critical analysis. *Can. J. Phys.* **1980,** 58 (8), 1200-1211; (d) Stephens, P. J.; Devlin, F. J.; Chabalowski, C. F.; Frisch, M. J., Ab Initio Calculation of Vibrational Absorption and Circular Dichroism Spectra Using Density Functional Force Fields. *J. Phys. Chem.* **1994,** 98 (45), 11623-11627.

(14) The computational protocol deemed to be optimal for the calculation of chemical shifts (vide infra) has been applied to generate all the data presented in this section.

(15) (a) Chesnut, D. B.; Moore, K. D., Locally dense basis sets for chemical shift calculations. *J. Comp. Chem.* **1989,** 10 (5), 648-659; (b) Chesnut, D. B.; Rusiloski, B. E.; Moore, K. D.; Egolf, D. A., Use of locally dense basis sets for nuclear magnetic resonance shielding calculations. *J. Comp. Chem.* **1993,** 14 (11), 1364-1375.

(16) The viability of this approach for the calculation of spin-spin coupling constants has also been examined, see: Provasi P. F.; Aucar G. A., *J. Chem. Phys.* **2000,** 112, 6201-6208 and Sanchez M.; Provasi P. F.; Aucar G. A.; Sauer S. P. A., *Adv. Quant. Chem.* **2005,** 48, 161-183. The concept proved valuable also in other contexts, such as the cost-effective prediction of bond dissociation enthalpies and other molecular properties see: DiLabio G. A., *J. Chem. Phys. A* **1999,** 103 (51), 11414-11424.

(17) Chesnut, D. B.; Byrd, E. F. C., The use of locally dense basis sets in correlated NMR chemical shielding calculations. *Chem. Phys.* **1996,** 213 (1), 153-158.

(18) (a) Reid, D. M.; Kobayashi, R.; Collins, M. A., Systematic Study of Locally Dense Basis Sets for NMR Shielding Constants. *J. Chem. Theor. Comp.* **2014,** 10 (1), 146-152; (b) Amos, R.; Kobayashi, R., Ab Initio NMR Chemical Shift Calculations Using Fragment Molecular Orbitals and Locally Dense Basis Sets. *J. Phys. Chemi. A* **2016,** 120 (44), 8907-8915.

(19) Jensen, F., Basis Set Convergence of Nuclear Magnetic Shielding Constants Calculated by Density Functional Methods. *J. Chem. Theor. Comp.* **2008,** 4 (5), 719-727.

(20) Zhang, Y.; Wu, A.; Xu, X.; Yan, Y., OPBE: A promising density functional for the calculation of nuclear shielding constants. *Chem. Phys. Lett.* **2006,** 421 (4), 383-388.

(21) (a) Bye, E.; Schweizer, W. B.; Dunitz, J. D., Chemical reaction paths. 8. Stereoisomerization path for triphenylphosphine oxide and related molecules: indirect observation of the structure of the transition state. *J. Am. Chem. Soc.* **1982,** 104 (22), 5893-5898; (b) Wille, E. E.; Stephenson, D. S.; Capriel, P.; Binsch, G., Iterative analysis of exchange-broadened NMR band shapes. The mechanism of correlated rotations in triaryl derivatives of phosphorus and arsenic. *J. Am. Chem. Soc.* **1982,** 104 (2), 405-415; (c) Brock, C. P.; Ibers, J. A., Conformational analysis of the triphenylphosphine molecule in the free and solid states. *Acta Cryst. B* **1973,** 29 (11), 2426-2433; (d) Davies, S. G.; Derome, A. E.; McNally, J. P., Conformational analysis and dynamics of the triphenylphosphine ligand in iron complex [(.eta.5-C₅H₅)Fe(CO)(PPh₃)COCH₃]. *J. Am. Chem. Soc.* **1991,** 113 (8), 2854-2861; (e) Fey, N.; Howell, J. A. S.; Lovatt, J. D.; Yates, P. C.; Cunningham, D.; McArdle, P.; Gottlieb, H. E.; Coles, S. J., A molecular mechanics approach to mapping the conformational space of diaryl and triarylphosphines. *Dalton Trans.* **2006,** (46), 5464-5475.

(22) Payard, P.-A.; Perego, L. A.; Ciofini, I.; Grimaud, L., Taming Nickel-Catalyzed Suzuki-Miyaura Coupling: A Mechanistic Focus on Boron-to-Nickel Transmetalation. *ACS Cat.* **2018,** 8 (6), 4812-4823.

(23) Passera, A.; Mezzetti, A., Mn(I) and Fe(II)/PN(H)P Catalysts for the Hydrogenation of Ketones: A Comparison by Experiment and Calculation. *Adv. Synth. Catal.* **2019,** 361 (20), 4691-4706.

(24) De Luca, L.; Passera, A.; Mezzetti, A., Asymmetric Transfer Hydrogenation with a Bifunctional Iron(II) Hydride: Experiment Meets Computation. *J. Am. Chem. Soc.* **2019,** 141 (6), 2545-2556.

(25) M. J. Frisch, G. W. Trucks, H. B. Schlegel, G. E. Scuseria, M. A. Robb, J. R. Cheeseman, G. Scalmani, V. Barone, B. Mennucci, G. A. Petersson, H. Nakatsuji, M. Caricato, X. Li, H. P. Hratchian, A. F. Izmaylov, J. Bloino, G. Zheng, J. L. Sonnenberg, M. Hada, M. Ehara, K. Toyota, R. Fukuda, J. Hasegawa, M. Ishida, T. Nakajima, Y. Honda, O. Kitao, H. Nakai, T. Vreven, J. A. Montgomery, Jr., J. E. Peralta, F. Ogliaro, M. Bearpark, J. J. Heyd, E. Brothers, K. N. Kudin, V. N. Staroverov, R. Kobayashi, J. Normand, K. Raghavachari, A. Rendell, J. C. Burant, S. S. Iyengar, J. Tomasi, M. Cossi, N. Rega, N. J. Millam, M. Klene, J. E. Knox, J. B. Cross, V. Bakken, C. Adamo, J. Jaramillo, R. Gomperts, R. E. Stratmann, O. Yazyev, A. J. Austin, R. Cammi, C. Pomelli, J. W. Ochterski, R. L. Martin, K. Morokuma, V. G. Zakrzewski, G. A. Voth, P. Salvador, J. J. Dannenberg, S. Dapprich, A. D. Daniels, Ö. Farkas, J. B. Foresman, J. V. Ortiz, J. Cioslowski, D. J. Fox, Gaussian, Inc., Wallingford CT, 2009.

(26) (a) Hay, P. J.; Wadt, W. R., Ab initio effective core potentials for molecular calculations. Potentials for the transition metal atoms Sc to Hg. *J. Chem. Phys.* **1985,** 82 (1), 270-283; (b) Wadt, W. R.; Hay, P. J., Ab initio effective core potentials for molecular calculations. Potentials for main group elements Na to Bi. *J. Chem. Phys.* **1985,** 82 (1), 284-298; (c) Hay, P. J.; Wadt, W. R., Ab initio effective core potentials for molecular calculations. Potentials for K to Au including the outermost core orbitals. *J. Chem. Phys.* **1985,** 82 (1), 299-310.

(27) (a) Tomasi, J.; Mennucci, B.; Cammi, R., Quantum Mechanical Continuum Solvation Models. *Chem. Rev.* **2005,** 105 (8), 2999-3094; (b) Cossi, M.; Scalmani, G.; Rega, N.; Barone, V., New developments in the polarizable continuum model for quantum mechanical and classical calculations on molecules in solution. *J. Chem. Phys.* **2002,** 117 (1), 43-54.